Available online at www.sciencedirect.com

ScienceDirect

Energy Procedia 70 (2015) 95 – 102

Energy Procedia

International Conference on Solar Heating and Cooling for Buildings and Industry, SHC 2014

Performance analysis and optimization of a vapor-filled flat-plate solar collector

Deodat Makhanlall*, Peixue Jiang

Tsinghua University, Key Laboratory for Thermal Science and Power Engineering of the Ministry of Education, Beijing 100084, PR China

Abstract

Solar thermal collectors are certain to play a primary role in reducing energy consumption in buildings. At present, significant efforts are being made to find new ways to enhance their performance. An emerging technique is studied in this work based on thermodynamic analysis. The study shows how thermodynamic 2nd-law analysis can be used to complement the 1st law analysis approach for a FPSC (flat-plate solar collector) in which the confined air in the spacing between the absorber and glass cover is replaced by water-vapor. In the analysis, the influence of key parameters such solar irradiation, inclination angle, as well as the use of absorbers with different emissivity values, are investigated.

Peer-review by the scientific conference committee of SHC 2014 under responsibility of PSE AG

Keywords: Filled flat-plate solar collector; thermodynamic analysis; computational fluid dynamics; optimization

1. Introduction

Low-temperature solar energy utilization systems are very interesting for meeting today's increasing domestic and industrial air-conditioning and heating demand. Flat-plate solar collectors (FPSC) are the primary components in most of these systems, and it has been a focus of research on renewable energy, with much study done for its heat transfer optimization. The methods for improving the performance of FPSC fall into two categories:

- Reducing the collector's convective and radiative heat losses
- Raising the collector's effective absorption of solar irradiation

* Corresponding author. Tel.: +86-10-62771415.
E-mail address: deodat@mail.tsinghua.edu.cn (D. Makhanlall)

Peer-review by the scientific conference committee of SHC 2014 under responsibility of PSE AG
doi:10.1016/j.egypro.2015.02.103

Nomenclature

A	wall surface area, m^2
$\dot{E}''_{loss}$	rate of convective and radiative thermal losses per unit surface area of the absorber, W m^{-2}
$\dot{E}''_R$	rate of solar energy absorption per unit surface area of the absorber, W m^{-2}
h_w	wind heat transfer coefficient, W m^{-2} K^{-1}
I_λ	spectral energy intensity of a radiation beam, W m^{-3} sr^{-1}
$I_{b\lambda}$	backbody spectral energy intensity of a radiation beam, W m^{-3} sr^{-1}
k	thermal conductivity of water vapor (air), W m^{-1} K^{-1}
L_λ	spectral entropy intensity of a radiation beam, W m^{-2} μm^{-1} sr^{-1} K^{-1}
N_S	entropy generation number
$\mathbf{n_w}$	unit outward normal vector of boundary wall
$\dot{Q}$	heat transfer rate, W
$\mathbf{r}$	unit position vector
$\mathbf{s}$	unit direction vector
$\dot{S}'''_{gen}$	total local rate of entropy generation, W m^{-3} K^{-1}
$\dot{S}'''_{gen,c}$	local rate of entropy generation due to heat conduction and convection, W m^{-3} K^{-1}
$\dot{S}'''_{gen,f}$	local rate of entropy generation due to viscous dissipation, W m^{-3} K^{-1}
$\dot{S}'''^{aes}_{gen,r}$	local rate of entropy generation due to absorption, emission and scattering in medium, W m^{-3} K^{-1}
$\dot{S}''^{w}_{gen,r}$	local rate of entropy generation due to radiation absorption and emission at solid surfaces, W m^{-2} K^{-1}
$\dot{S}_{gen}$	global rate of entropy generation, W K^{-1}
T	temperature, K
T_0	temperature of reference environment, 300K
T_c, T_h	temperature of cold surface and hot surface respectively, K
T_{pm}, T_p	mean and local temperature of absorber plate, K
T_λ	spectral radiation temperature, K
U_t	top heat loss coefficient, W m^{-2} K^{-1}
V	volume, m^{-3}
β	the collector's inclination angle, degrees
ε_g	emissivity of glass cover
ε_p	emissivity of absorber plate
κ_a	absorption coefficient, m^{-1}
κ_s	scattering coefficient, m^{-1}
λ	wavelength, m^{-1}
μ	dynamic viscosity of water vapor (air), kg m^{-1} s^{-1}
σ	Stefan–Boltzmann constant, W m^{-2} K^{-4}
Φ	scattering phase function
Π_{gen}	dimensionless entropy generation rate
Ω	solid angle, sr
Ψ	viscous dissipation function, s^{-2}

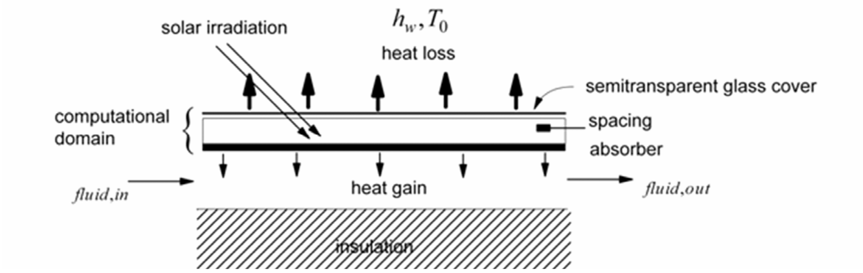

Fig. 1. Schematic of flat-plate solar collector with problem domain

The heat loss reduction methods are most suitable for FPSCs [1], and a novel approach in this category is gas-filling. Replacing the air in the spacing between the absorber and glass cover of a FPSC with certain gasses is a promising technique for reducing the heat losses [2]. However, the gas-filling approach is an emerging method that requires much more research before being implemented as a standard design concept with high customer's confidence.

The objective of this work is to evaluate the thermodynamic performance of a FPSC that uses water-vapor to capture solar energy. The analysis is based on the laws of thermodynamics, and is carried out with the computational fluid dynamics code FLUENT® 6.3. The problem domain is shown in Fig. 1, and involves the confined natural flow of vapor in a model FPSC. The study is limited to Raleigh numbers smaller than 5×10^4. For such conditions, 2D laminar flow can be assumed to exist [3].

2. The thermodynamics of flat-plate solar collectors

2.1. Energy and entropy flows

The performance of a FPSC is described by an energy balance, depicted in Fig. 2a, showing the distribution of the incident solar energy into useful energy gain and thermal losses. The losses, due to the conduction, convection and thermal radiation across the absorber-glass cover spacing can be written as:

$$\dot{E}''_{loss} = U_t\left(T_{pm} - T_0\right) \tag{1}$$

For single-glazed FPSCs, the equation commonly used for U_t (the heat loss coefficient) is [4]:

$$U_t = \left\{\left(\frac{C}{T_{pm}}\right)^{-1}\left[\frac{T_{pm} - T_0}{1+f}\right]^{-e} + \frac{1}{h_w}\right\}^{-1} + \frac{\sigma\left(T_{pm} + T_0\right)\left(T_{pm}^2 + T_0^2\right)}{\left(\varepsilon_p + 0.00591 h_w\right)^{-1} + \frac{1 + f + 0.133\varepsilon_p}{\varepsilon_g} - 1} \tag{2}$$

where,

$$C = 520\left(1 - 0.000051\beta^2\right)\text{for } 0^0 < \beta < 70^0.70^0 < \beta < 90^0.\text{For } \beta = 70^0. \tag{3}$$

$$e = 0.430\left(1 - 100/T_{pm}\right) \tag{4}$$

$$f = 1.007866 \times \left(1 + 0.089 h_w - 0.1166 h_w \varepsilon_p\right) \tag{5}$$

$$T_{pm} = \frac{1}{A}\int T_p dA \tag{6}$$

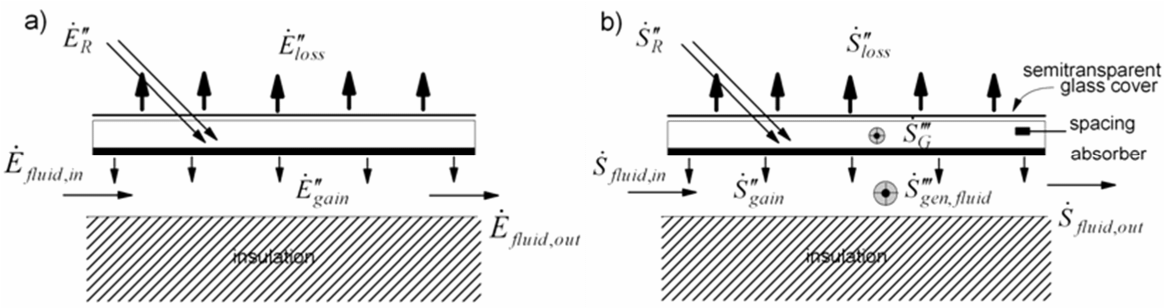

Fig. 2. (a) energy flow, and (b) entropy flow and entropy generation in FPSCs.

The energy flow in a collector is accompanied by a flow of entropy (Fig. 2b). Unlike energy, entropy is not conserved. Entropy is generated in the transport fluid and in the medium between the absorber and cover. Entropy generation in the transport fluid has been studied [5-8]). This paper focuses on entropy generation in the spacing.

2.2. Entropy generation

Entropy generation in the spacing between the absorber and glass cover is closely linked to the driving force of the thermal losses in a FPSC. A collector's thermal losses usually become very significant when a large temperature difference exists between the absorber and glass cover [4]. From a thermodynamic point of view, the temperature difference corresponds to an irreversible phenomenon which involves entropy generation. Thus, with increase of temperature difference, not only does the energy flow increase, but also the flow of entropy and the rate of entropy generation. Through entropy generation minimization techniques, the thermal losses from a FPSC can be managed.

In the spacing, entropy generation is due to the irreversibilities associated with the natural convection and thermal radiation processes. The overall rate of entropy generation in the spacing can be written as following [9]:

$$\dot{S}_{gen} = \dot{S}_{gen,f} + \dot{S}_{gen,c} + \dot{S}^{aes}_{gen,r} + \dot{S}^{w}_{gen,r} \tag{7}$$

where,

$$\dot{S}'''_{gen,f} = \mu\Psi/T \tag{8}$$

$$\dot{S}'''_{gen,c} = k(\nabla T)^2/T^2 \tag{9}$$

$$\begin{aligned}\dot{S}'''^{aes}_{gen,r} = &\int_0^\infty \int_{4\pi} \left[-(\kappa_a + \kappa_s)\frac{I_\lambda(\mathbf{r},\mathbf{s})}{T_\lambda(\mathbf{r},\mathbf{s})} + \kappa_a \frac{I_{b\lambda}(\mathbf{r})}{T_\lambda(\mathbf{r},\mathbf{s})} + \frac{\kappa_s}{4\pi}\int_{4\pi} \frac{I_\lambda(\mathbf{r},\mathbf{s}')}{T_\lambda(\mathbf{r},\mathbf{s})}\Phi_\lambda(\mathbf{s},\mathbf{s}')\mathrm{d}\Omega' \right]\mathrm{d}\Omega'\mathrm{d}\lambda \\ &+ \int_0^\infty \int_{4\pi} \kappa_a \frac{I_\lambda(\mathbf{r},\mathbf{s}) - I_{b\lambda}(\mathbf{r})}{T(\mathbf{r})}\mathrm{d}\Omega\mathrm{d}\lambda\end{aligned} \tag{10}$$

$$\dot{S}''^{w}_{gen,r} = \int_0^\infty \int_{4\pi} \left[I_\lambda(\mathbf{r}_w,\mathbf{s})/T(\mathbf{r}_w) - L_\lambda(\mathbf{r}_w,\mathbf{s})|\mathbf{n_w}\cdot\mathbf{s}|\mathrm{d}\Omega\mathrm{d}\lambda \right] \tag{11}$$

$$\dot{S}_{gen,f} = \int_V \dot{S}'''_{gen,f}\mathrm{d}V \tag{12}$$

$$\dot{S}_{gen,c} = \int_V \dot{S}'''_{gen,c}\mathrm{d}V \tag{13}$$

$$\dot{S}^{aes}_{gen,r} = \int_V \dot{S}'''^{aes}_{gen,r}\mathrm{d}V \tag{14}$$

$$\dot{S}^{w}_{gen,r} = \int_A \dot{S}'''^{w}_{gen,r}\mathrm{d}A \tag{15}$$

Eq. (8) and Eq. (9) are treated in detail in [10], while Eq. (10) and Eq. (11) are discussed [11] and [12].

2.3. Entropy generation number

The thermodynamic second-law performance of the FPSC can be evaluated using the entropy generation number given by Eq. (16). The entropy generation number represents the fraction of the captured solar radiant energy that is not utilized due to the collector's internal thermodynamic irreversibilities.

$$N_S = N_{S,f} + N_{S,c} + N^{aes}_{S,r} + N^{w}_{S,r} = T_0\dot{S}_{gen} \Big/ \int \dot{E}''_R dA \tag{16}$$

with

$$N_{S,f} = \frac{T_0\dot{S}_{gen,f}}{\int \dot{E}''_R dA};\ N_{S,c} = \frac{T_0\dot{S}_{gen,c}}{\int \dot{E}''_R dA};\ N^{aes}_{S,r} = \frac{T_0\dot{S}^{aes}_{gen}}{\int \dot{E}''_R dA};\ N^{w}_{S,r} = \frac{T_0\dot{S}^{w}_{gen}}{\int \dot{E}''_R dA} \tag{17}$$

3. Results and discussion

3.1. Model validation

The numerical model was validated based on classical thermodynamic theorem. For combined convection and radiation heat transfer in an enclosure, the overall rate of entropy generation is defined as following:

$$\dot{S}_{gen}\left(\text{theoretical}\right) = \dot{Q}_{tot}\left(T_c^{-1} - T_h^{-1}\right) \tag{18}$$

The numerical value computed using Eq. (7) should clearly be equal to the theoretical value obtained with Eq. (18). In dimensionless form, the following relations can be written:

$$\Pi_{gen}\left(\text{theoretical}\right) = \dot{S}_{gen}\left(\text{theoretical}\right)T_c \big/ \dot{Q}_{tot} = 1 - T_c/T_h \tag{19}$$

$$\Pi_{gen}\left(\text{numerical}\right) = \Pi_f + \Pi_c + \Pi^{aes}_r + \Pi^{w}_r \tag{20}$$

with

$$\Pi_f = \dot{S}_{gen,f}T_c \big/ \dot{Q}_{tot};\ \Pi_c = \dot{S}_{gen,c}T_c \big/ \dot{Q}_{tot};\ \Pi^{aes}_r = \dot{S}^{aes}_{gen,r}T_c \big/ \dot{Q}_{tot};\ \Pi^{w}_r = \dot{S}^{w}_{gen}T_c \big/ \dot{Q}_{tot} \tag{21}$$

The validation model is shown in Fig. 3a. Entropy generation due to natural convection-radiation interaction in an enclosure filled with water vapor is considered. The vapor is treated as an absorbing, emitting and scattering gas with $\kappa_a = 0.54m^{-1}$ and $k_s = 0.01m^{-1}$. Other thermophysical properties are taken from FLUENT Database. The wall emissivity is varied to test the model and assess the role of radiation. As shown in Fig. 3b, the dimensionless overall entropy generation rate has a theoretical value of 1-300/400 = 0.25. The predicted conduction and radiation entropy generation rates also sum up to 0.25. In addition, it can be seen that the thermodynamic second-law role of thermal radiation is very important in the operating temperature range of FPSC, while entropy generation due to viscous dissipation can be neglected.

Grid independence study was performed by adapting the grid in high-gradient zones. Results were considered independent when the change in entropy generation rate was less than 1%. The final grid consisted of 2500 cells.

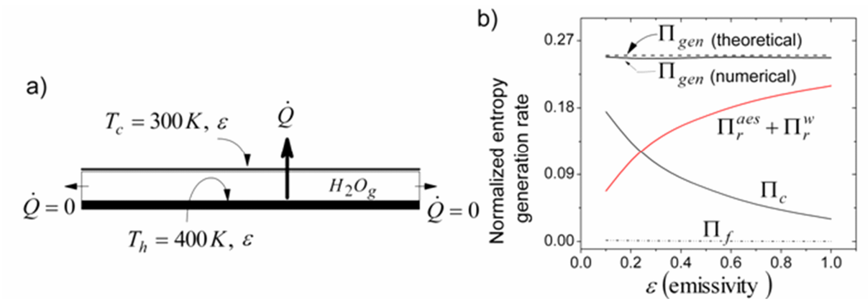

Fig. 3. (a) validation model with (b) normalized entropy generation rates.

3.2. Irradiation characteristics

Solar collectors operate under variable energy fluxes, and, at best, the incident solar irradiation of a FPSC is about 1100 W/m^2 [4]. For irradiation in the range 500-1200 W/m^2, Fig. 4 shows the absorber mean temperature, thermal losses, and entropy generation number of the vapor-filled collector. The absorber heats up more as it receives more energy and, as the temperature difference over the vapor layer becomes larger, the convective and radiative heat losses increases. Entropy generation in de vapor layer is closely linked to the collector's thermal losses. The entropy generation number increases, in the same trend as the losses, with increasing irradiation flux. This means that a lower fraction of the incident solar energy is utilized at a higher irradiation flux. From the inset Table in Fig. 4, it can be seen that the radiation entropy generation number is much larger than the convection entropy generation number at a high irradiation flux. Thus, thermal radiation is the main cause of the collector's losses under such conditions. At a low irradiation flux, however, the entropy generation numbers of convection and radiation are about the same value, indicating that radiation and convection losses are both equally important.

3.3. Influence of absorber emissivity

The irradiation characteristics in Fig. 4 do not show significant improvement from what would be expected from an air-filled collector. With air-filled FPSC, 100 K above ambient temperature can readily be achieved. However, given the significant impact of wall radiation processes (relatively high wall radiation entropy generation number), the absorber emissivity may offer a suitable way for managing thermal losses in vapor-filled FPSCs (see Fig. 5).

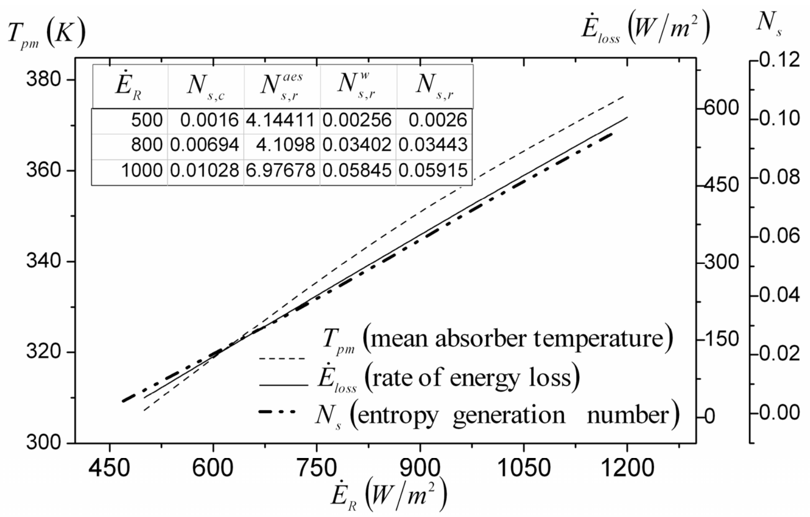

$\dot{E}_R$	$N_{s,c}$	$N_{s,r}^{aes}$	$N_{s,r}^{w}$	$N_{s,r}$
500	0.0016	4.14411	0.00256	0.0026
800	0.00694	4.1098	0.03402	0.03443
1000	0.01028	6.97678	0.05845	0.05915

Fig. 4. Vapor-filled FPSC characteristics at different irradiation flux.

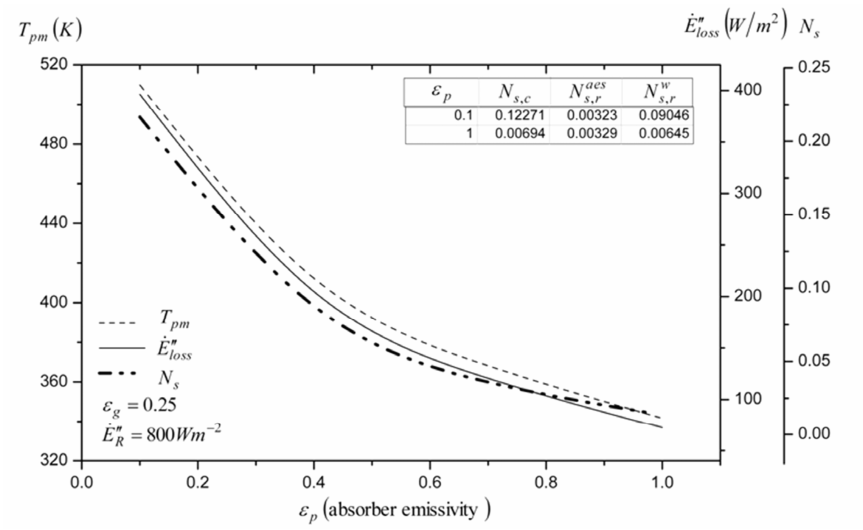

Fig. 5. Vapor-filled FPSC characteristics at different absorber emissivity.

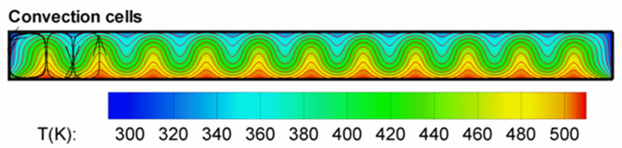

Fig. 6. Temperature field and convection cells in the spacing when the absorber emissivity is reduced to 0.2.

The absorber emissivity has significant effect on the performance of the vapor-filled FPSC. As shown in Fig.5, the absorber mean temperature, thermal losses, and entropy generation number increases when the absorber emissivity is reduced. The combination of a low emissivity cover and high emissivity absorber is estimated to have the best performance. The inset Table of conduction and radiation entropy generation number may provide an explanation for this. As can be seen from the inset Table, the radiation entropy generation number is larger than the conduction entropy generation number for the high-e absorber. However, the conduction entropy generation number becomes larger for the low-e absorber. Thus, while radiation is most important for the high-e absorber, convection becomes more important at the low-e absorber. The temperature field and convection cells are shown in Fig. 6 for absorber emissivity 0.2.

3.4. Influence of inclination angle

Analysis of a collector's performance at different inclination angle helps to determine the geographic location where the collector will have its best performance. The optimum angle for FPSC is approximately equal to the latitude. The performance of the vapor-filled FPSC as function of inclination angle is depicted in Fig. 7. The absorber mean temperature, thermal losses, and entropy generation number are minimal at zero degree inclination. These results are different than what is usually found for air-filled FPSC. Standard air-filled FPSC tend to have their best performance at a high degree of inclination [4]. The vapor-filled FPSC behave different than their air-filled counterparts most likely due to a stronger effect of radiation. As can be seen from the inset Table in Fig. 7, while the convection entropy generation number is not significantly affected by inclination, the radiation entropy generation number increases relatively strong. Thus, the influence of thermal radiation is felt much stronger as the inclination angle is increased in the vapor-filled FPSC.

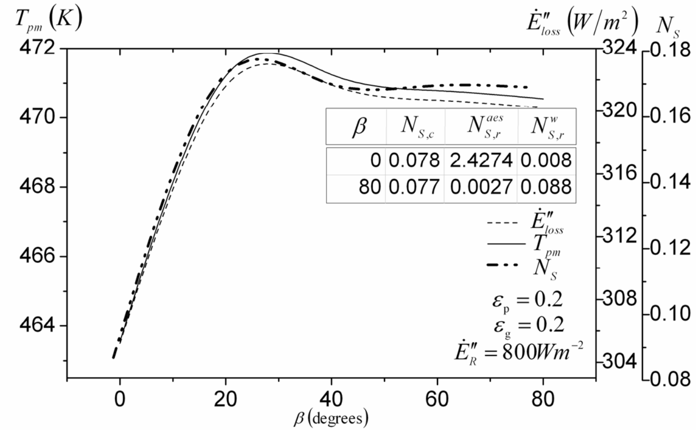

Fig. 7. Vapor-filled FPSC characteristics at different inclination angle.

4. Conclusions

Thermodynamic analysis has been carried out for an emerging class of FPSC (flat-plate solar collector). Here, the performance of a FPSC in which the confined air is replaced by water-vapor is studied. The analysis is based on the standard thermodynamic method, as well as a novel second-law approach. In addition, the influence of primary variables, such as the irradiation intensity, absorber emissivity, and inclination angle, are studied. Several important conclusions can be derived from this study, including:

- The performance of FPSC can best be understood and improved when the standard thermodynamic method is combined with second-law analysis
- The absorber emissivity has a very strong effect on the performance of vapor-filled FPSC. When the absorber emissivity is low, convection cells are formed in the confined spacing which leads to strong convections losses. Losses due to radiative heat transfer processes become more important with increasing absorber emissivity.
- The performance of vapor-filled FPSC improves when: a) irradiation intensity is low, absorber emissivity is high and class cover emissivity is low, the inclination angle is low

Acknowledgements

The authors gratefully acknowledge the support of this work by Tsinghua University.

References

[1] Sen Z. Solar energy fundamentals and modelling techniques: atmosphere, environment, climate change and renewable energy. London: Springer; 2008.
[2] Vestlund J, Dalenbäck JO, Rönnelid M. Thermal and mechanical performance of sealed, gas-filled solar collectors. Sol Energy 2012;86:13-25.
[3] Incropera FP, DeWitt DP, Bergman TL, Lavine AS. Fundamentals of heat and mass transfer. 6rd ed. New York: John Wiley; 2007.
[4] Duffie JA, Beckman WA. Solar engineering of thermal processes. 3rd ed. New York: Wiley; 2006.
[5] Saha SK, Mahanta DK. Thermodynamic optimization of solar flat-plate collector. Renew Energy 2001;23:181-193.
[6] Badescu V. Optimal control of flow in solar collectors for maximum exergy extraction. Int J Heat Mass Transf 2007;50:4311-4322.
[7] Farahat S, Sarhaddi F, Ajam H. Exergetic optimization of flat plate solar collectors. Renew Energy 2009;34:1169-1174.
[8] Pons M. Exergy analysis of solar collectors, from incident radiation to dissipation. Renew Energy 2012;47:194-202.
[9] Makhanlall D, Munda JL, Jiang P. Entropy generation in a solar collector filled with a radiative participating gas. Energy 2013;60:511-516.
[10] Bejan A. Entropy generation minimization. New York: CRC Press; 1996.
[11] Caldas F, Semiao V. Entropy generation through radiative transfer in participating media: analysis and numerical computation. J Quant Spectrosc Radiat Trans 2005;96:423-437.
[12] Liu LH, Chu SX. Verification of numerical simulation method for entropy generation of radiation heat transfer in semitransparent medium. J Quant Spectrosc Radiat Trans 2007;103:43-56.